Supporting Documents

In an effort to establish chemical makeup resulting from the synthesis of N-acryloyl-N′-propylpiperazine (AcrNPP) and 2-ethoxyethyl methacrylate (EEMA) monomers, ATR FT-IR analysis was performed. Figure S1, Traces A-E illustrate ATR FT-IR spectra of p(AcrNPP/EEMA) copolymers with the following compositions: AcrNPP:EEMA=1:9 (trace A), AcrNPP:EEMA=2:8 (trace B), AcrNPP:EEMA=3:7 (trace C), AcrNPP:EEMA=4:6 (trace D), and AcrNPP:EEMA=5:5 (trace E). As seen, the characteristic bands[1-6] due to AcrNPP at 2931 (CH_2 asym str), 2820-2760 (N-CH_2), 1642 (C=O, amide I), 1445 (C-H def), and 1050-980 (ring skeletal vib) cm^{-1} increase as the wt% of AcrNPP increase. The 1730 and 1120 cm^{-1} bands due to C=O ester and C-O-C stretching vibrations of EEMA[7, 8] are also observed for all the compositions, which significantly decreases as the copolymer composition changes from AcrNPP:EEMA=1:9 to AcrNPP:EEMA=5:5.

Figure S2, Traces A-E, illustrate ATR FT-IR spectra of p(VCl/nBA) copolymers with the following compositions: VCl:nBA=1:9 (trace A), VCl:nBA=2:8 (trace B), VCl:nBA=3:7 (trace C), VCl:nBA=4:6 (trace D), and VCl:nBA=5:5 (trace E). As seen, the band due to VCl[4, 6, 9] at 2931 (CH_2 asym str), 2854 (CH_2 sym str) cm^{-1} in the C-H stretching region as well as the 1638 (C=O, amide I), 1476 (CH_2), 1438, 1418 (CH_2 scissor), 1262 (C-N, amide III), and 974 (lactam ring) cm^{-1} increase as the wt% of VCl increase. The 1732 C=O and 1165 cm^{-1} due to C=O ester and C-O-C stretching vibrations of nBA[10] are detected for all the compositions, which gradually decrease going from Trace A to E.

Figure S3, Traces A-E, illustrate ATR FT-IR spectra of p(NIPMAM/nBA) copolymers with the following compositions: NIPMAm:nBA=1:9 (trace A), NIPMAm:nBA=2:8 (trace B), NIPMAm:nBA=3:7 (trace C), NIPMAm:nBA=4:6 (trace D), and NIPMAm:nBA=5:5 (trace E). As seen, the characteristic band due to NIPMAm[4, 6, 11] at 3600-3250 (N-H str), 1635 (C=O, amide I), 1528 (N-H, amide II), and 1385, 1369 (isopropyl) cm^{-1} increase as the amount of NIPMAm increase. The bands of nBA[10] at 1732 C=O and 1165 cm^{-1} due to C=O ester and C-O-C stretching vibrations are also observed for all compositions.

Figure S4, Traces A-E, illustrate ATR FT-IR spectra of p(DMAEMA/nBA) copolymers with the following compositions: DMAEMA:nBA=1:9 (trace A), DMAEMA:nBA=2:8 (trace B), DMAEMA:nBA=3:7 (trace C), DMAEMA:nBA=4:6 (trace D), and DMAEMA:nBA=5:5 (trace E). As seen, the characteristic bands of DMAEMA[12-14] at 2931 (CH_2 asym str) and 2854 (CH_2 sym str) cm^{-1} in the C-H stretching region as well as the 1566 (C-N str) and 1350-1500 (CH_2/CH_3 def) cm^{-1} bands due to aminoethyl groups increase as the DMAEMA content increases. Although, the carbonyl ester and C-O-C stretching bands of nBA and DMAEMA overlap, the characteristic broadening and a shift of the band at 1728 and 1161 cm^{-1} confirms the copolymerization.

In order to determine which molecular entities are responsible for the T_{SR} transitions, ATR FT-IR, Raman, and solid state ^{13}C NMR measurements are performed as a function of temperature. The analysis results of p(AcrNPP/EEMA) copolymer films are illustrated in Figure S5. As seen in Figure S5-A, the bands at 3000-2840 (C-H

str), 2820-2760 (>N-CH_2), 1642 (C=O amide I), 1445 (C-H def), 1235 (asym CCN), and 1050-980 (ring skeletal vib) cm^{-1} decrease significantly faster above 30 °C. The Raman analysis results illustrated in Figure S5-B exhibit the same phenomenon, in which the bands at 2935 (CH_2 asym), 2875 (CH_3 sym), 1452 (C-H def), 1291 (C-N ring), 1204 (CNC sym), and 1050-980 (ring C-C skeletal vib) cm^{-1} decrease at elevated temperature. Based on these analyses, the band intensity changes are mainly attributed to the C-H vibrations in the backbone/side groups as well as the amide and propylpiperazine functional groups of the AcrNPP component. Figure S5-C illustrate a series of ^{13}C NMR spectra with the characteristic resonances at 15.8 (-$OCH_2\mathbf{CH_3}$), 20.4 (-C-$\mathbf{CH_3}$), 45.6 (-**C**-), 55.5 (-COO-$\mathbf{CH_2}$), and 67.2 ppm ($\mathbf{CH_2}$-O-$\mathbf{CH_2}$) of EEMA, as well as at 12.4 (N-$(CH_2)_2$-$\mathbf{CH_3}$), 30.8 (-CH_2-**CH**-), 53.7 (N-$\mathbf{CH_2}$-CH_2), and 67.1 ppm (N-$\mathbf{(CH_2)_4}$-N) of AcrNPP. As anticipated, the copolymer chains will rearrange from the extended to collapse states when temperature increases, which will consequently affect the resonance intensities. However, the NMR analysis is not as pronounced as IR and Raman measurements for p(AcrNPP/EEMA).

ATR FT-IR, Raman, and ^{13}C NMR spectra of p(VCl/nBA) copolymers are summarized in Figure S6, A, B, and C, respectively. As shown in Figure 6-A, significant intensity decrease of the 2931 (CH_2 asym), 1438 (CH_2 scissoring), 1262 (C-N amide III), and 974 (lactam ring) cm^{-1} bands are observed as temperature increases. Moreover, the C=O amide I linkage at 1638 becomes narrower and shifts to 1645 cm^{-1} above 30 °C as illustrated in the 1780-1600 cm^{-1} region of insert a. Figure S6-B illustrates the Raman spectra and the bands at 2936 (CH_2 asym), 1446 (C-H def),

1085 (CH_2 sym def), 1030 (C-H ring), 840, 800 (sym CNC), and 696, 674 (lactam N-C=O) cm^{-1} also decreases as the temperature increases. These data indicate that the C-H vibrations in the backbone/side groups as well as the amide and lactam ring vibrations of the VCl component are responsible for the T_{SR} transitions. To further justify these conclusions solid state ^{13}C NMR measurements were performed, and the results are illustrated in Figure S6-C. As seen, the resonances at 24.5, 31.3, and 39.6 ppm due to lactam ring as well as the backbone resonances at 36.5, 41.6, and 41.6 ppm exhibit a significant decrease at elevated temperatures, which again supports the IR and Raman results.

Figure S7-A illustrates ATR FT-IR spectra of p(NIPMAm/nBA) copolymer films recorded as a function of temperature. As seen, the bands at 1635 (C=O amide I), 1528 (N-H amide II), 1460 (CH_3 def) and 1385, 1369 (C-H) in the 1850-1280 cm^{-1} region decrease as temperature increases. At the same time, the selected –C=O and N-H bands shift from 1635 to 1643 and 1528 to 1517 cm^{-1} above 35 °C, which reflect the molecular rearrangements in –C=O and N-H functionalities. Upon temperature increase, partial inter-molecular H-bonds gradually break down to generate intra-molecular H-bonds, which are manifested by the intensity increase of the 1660 cm^{-1} band. Insert a in Figure S7-A illustrates the N-H (3458, 3406, 3356) and C-H (3000-2850) stretching vibrations in 3720-2800 cm^{-1} region, which again exhibit significant intensity decrease at above 35 °C. These results indicate that the C-H vibrations and the amide and isopropyl functional groups of NIPMAm are responsible for molecular rearrangements at the T_{SR} transition, which are also confirmed in the

Raman measurements (Figure S7-B) manifested by the intensity decrease of the bands at 2930 (CH_2 asym), 1452 (C-H asym def), 1158, 1129 (C-C), and 847 (CNC str) cm^{-1}. Also, the 1379 and 1350 (C-H sym def) bands increase indicating that the C-H vibrations of $–CH(CH_3)_2$ entities become more symmetric at elevated temperatures. Figure S7-C illustrate ^{13}C NMR spectra of p(NIPMAm/nBA) with characteristic resonances of isopropyl groups at 19.0 and 41.6 ppm as well as the backbone resonances at 31.0, 40.3, and 45.6 ppm. As temperature increases, the intensity of these peaks decrease confirming again that the C-H, amide, and isopropyl entities are responsible for the T_{SR} transition in p(NIPMAm/nBA).

Figure S8, A, B, and C illustrate ATR FT-IR, Raman and ^{13}C NMR spectra of p(DMAEMA/nBA) copolymer films recorded as a function of temperature. As seen, in Figure 8-A, the C-H stretching vibrations at 2931 (CH_2 asym str), 2854 (CH_2 sym str) as well as the C-N stretching and C-H deformation bands at 1566, 1466, and 1401, 1382 cm^{-1} decrease significantly faster above 32 °C. Similar results are observed in the Raman measurements with the bands at 2931 (CH_2 asym str), 1453 (C-H def), 1405 (sym CH_3 def), 1300 (CH_3 rock/CCN str), 843 (CNC str) and 778 (C-N amine) cm^{-1} being weaker at elevated temperatures. ^{13}C NMR spectra shown in Figure 8-C illustrate that the resonances due to dimethylamino ethyl at 53.6, 57.4, 60.0 ppm as well as the backbone peaks at 43.7 and 17.2 ppm decrease above 32 °C. The NMR results combined with IR and Raman analysis indicate the intensities decrease is mainly attributed to the C-H vibration from copolymer backbone/side groups and dimethylamino ethyl functional groups of the DMAEMA component.

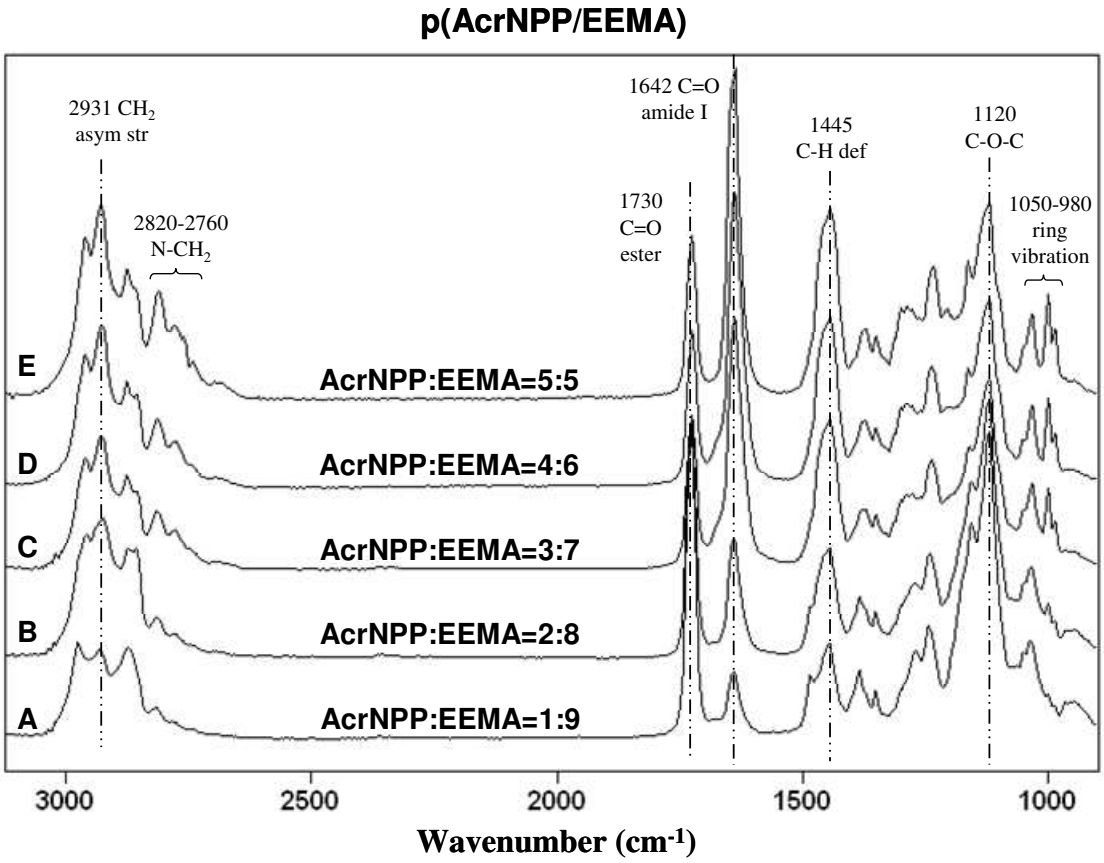

Figure S1. ATR FT-IR spectra of p(AcrNPP/EEMA) recorded as a function of copolymer composition: A-AcrNPP:EEMA=1:9; B-AcrNPP:EEMA=2:8; C-AcrNPP:EEMA=3:7; D-AcrNPP:EEMA=4:6; E-AcrNPP:EEMA=5:5.

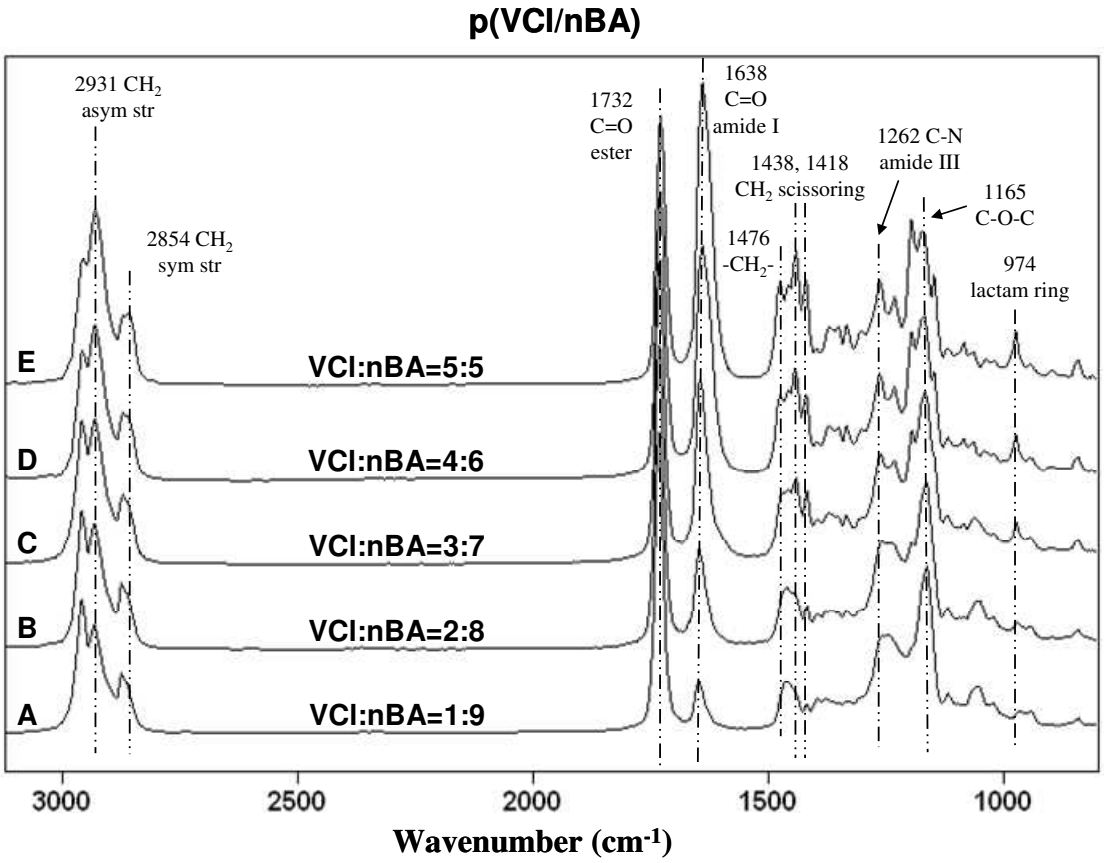

Figure S2. ATR FT-IR spectra of p(VCl/nBA) recorded as a function of copolymer composition: A-VCl:nBA=1:9; B-VCl:nBA=2:8; C-VCl:nBA=3:7; D-VCl:nBA=4:6; E-VCl:nBA=5:5.

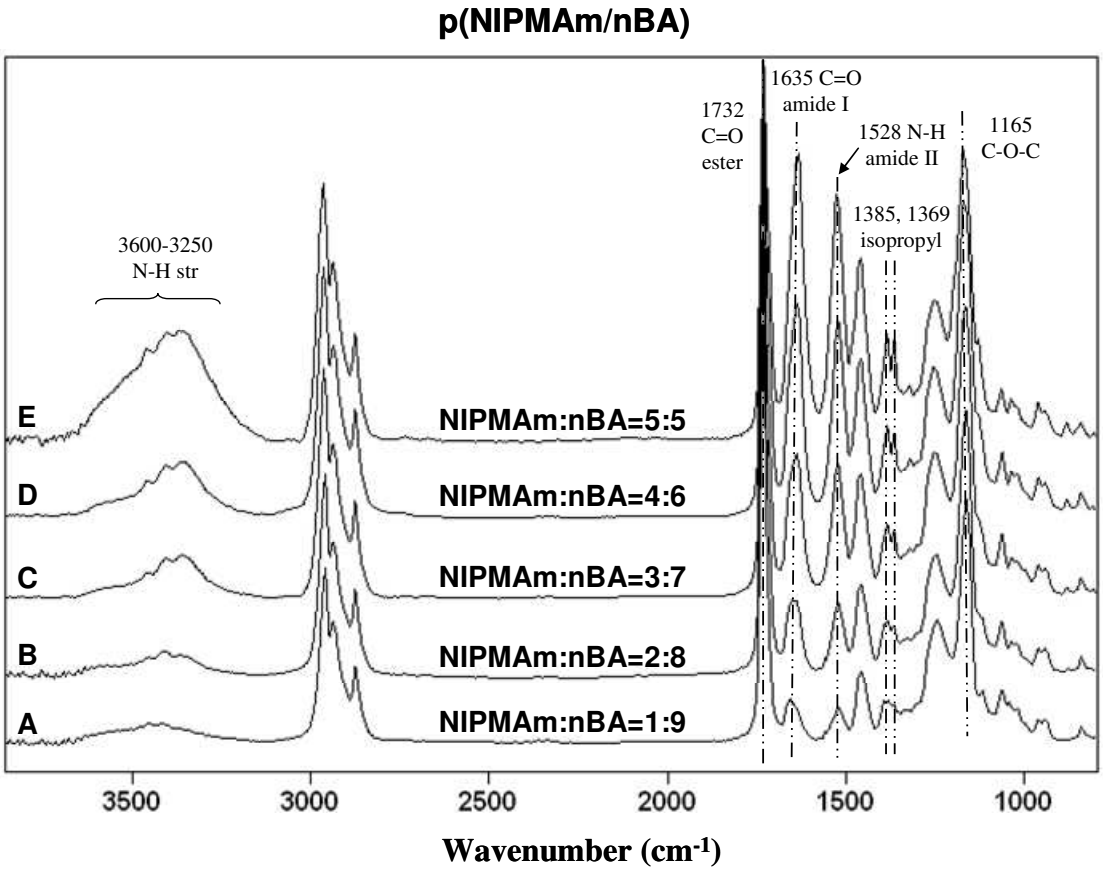

Figure S3. ATR FT-IR spectra of p(NIPMAm/nBA) recorded as a function of copolymer composition: A-NIPMAm:nBA=1:9; B-NIPMAm:nBA=2:8; C-NIPMAm:nBA=3:7; D-NIPMAm:nBA=4:6; E-NIPMAm:nBA=5:5.

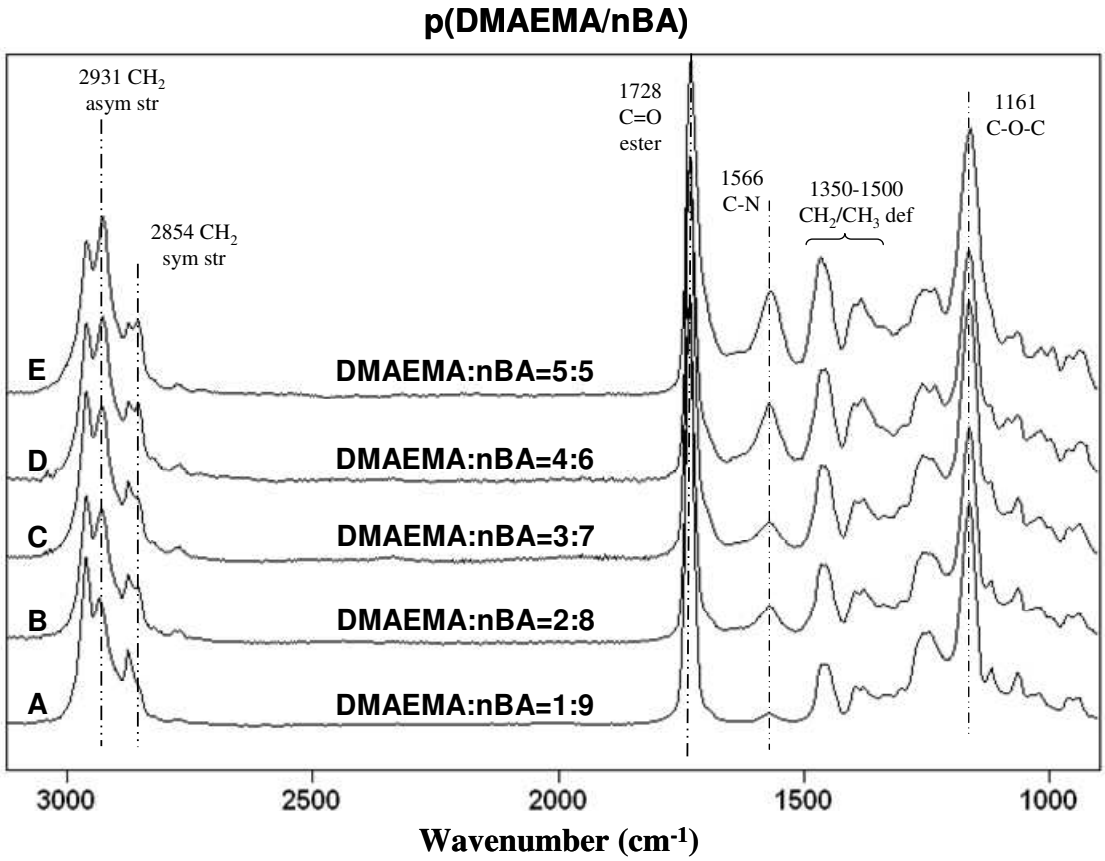

Figure S4. ATR FT-IR spectra of p(DMAEMA/nBA) recorded as a function of copolymer composition: A-DMAEMA:nBA=1:9; B-DMAEMA:nBA=2:8; C-DMAEMA:nBA=3:7; D-DMAEMA:nBA=4:6; E-DMAEMA:nBA=5:5.

A IR Spectra of p(AcrNPP/EEMA) as a Function of Temperature

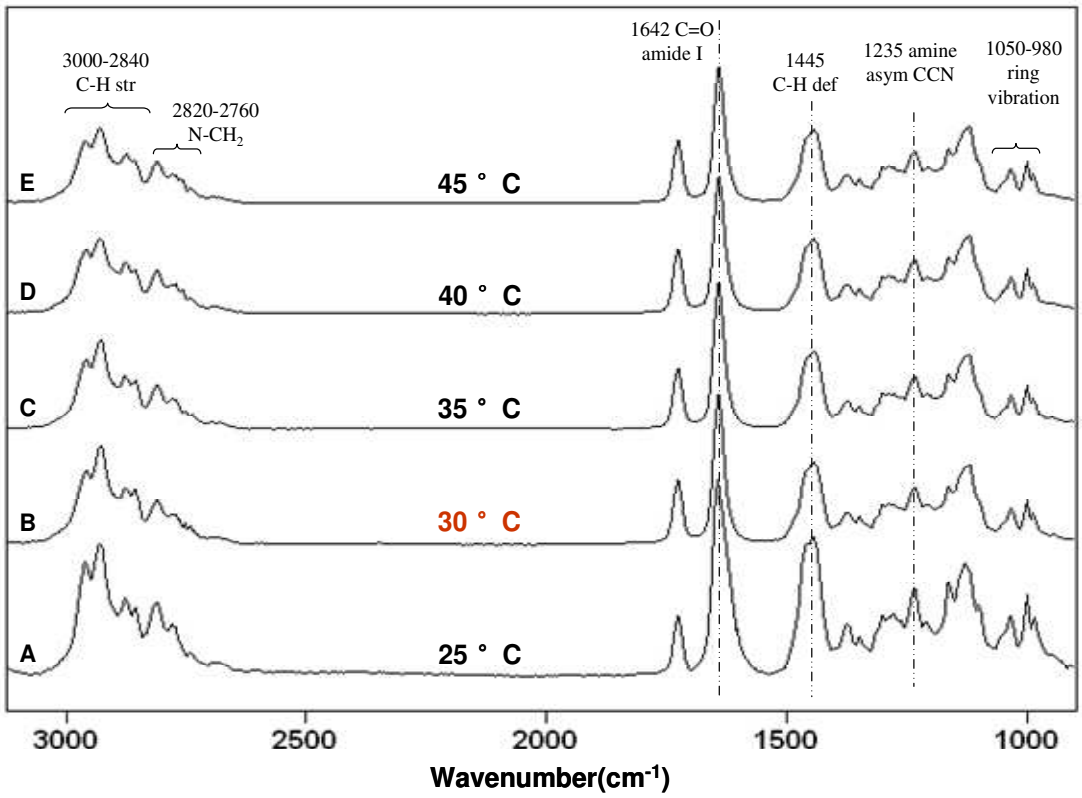

B Raman Spectra of p(AcrNPP/EEMA) as a Function of Temperature

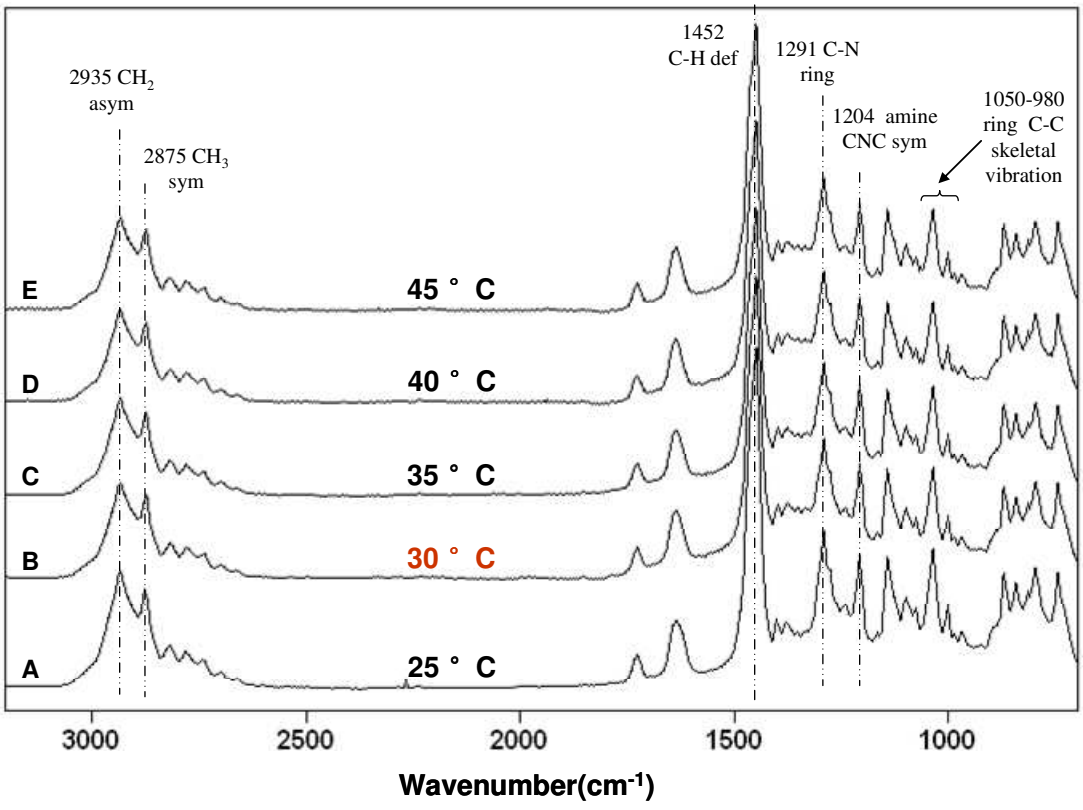

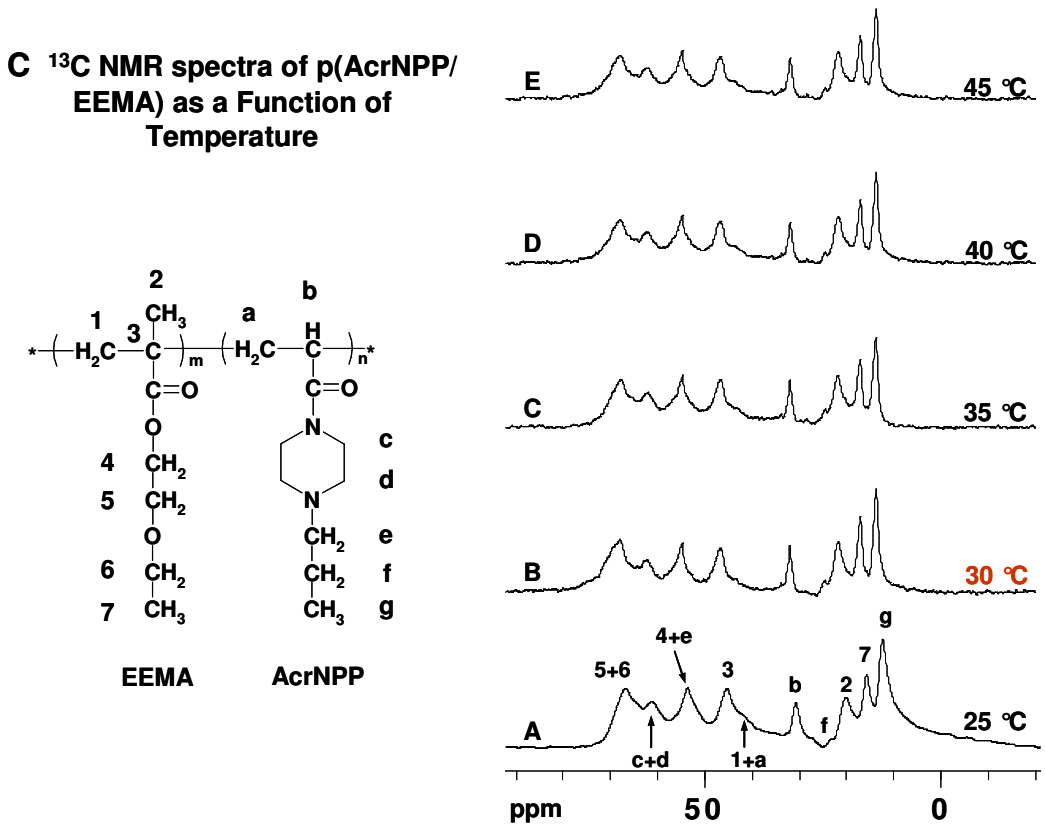

Figure S5. ATR FT-IR (A), Raman (B), and solid state ^{13}C NMR (C) spectra of p(AcrNPP/EEMA) recorded as a function of temperature; A-25 °C; B-30 °C; C-35 °C; D-40 °C; E-45 °C.

A IR Spectra of p(VCl/nBA) as a Function of Temperature

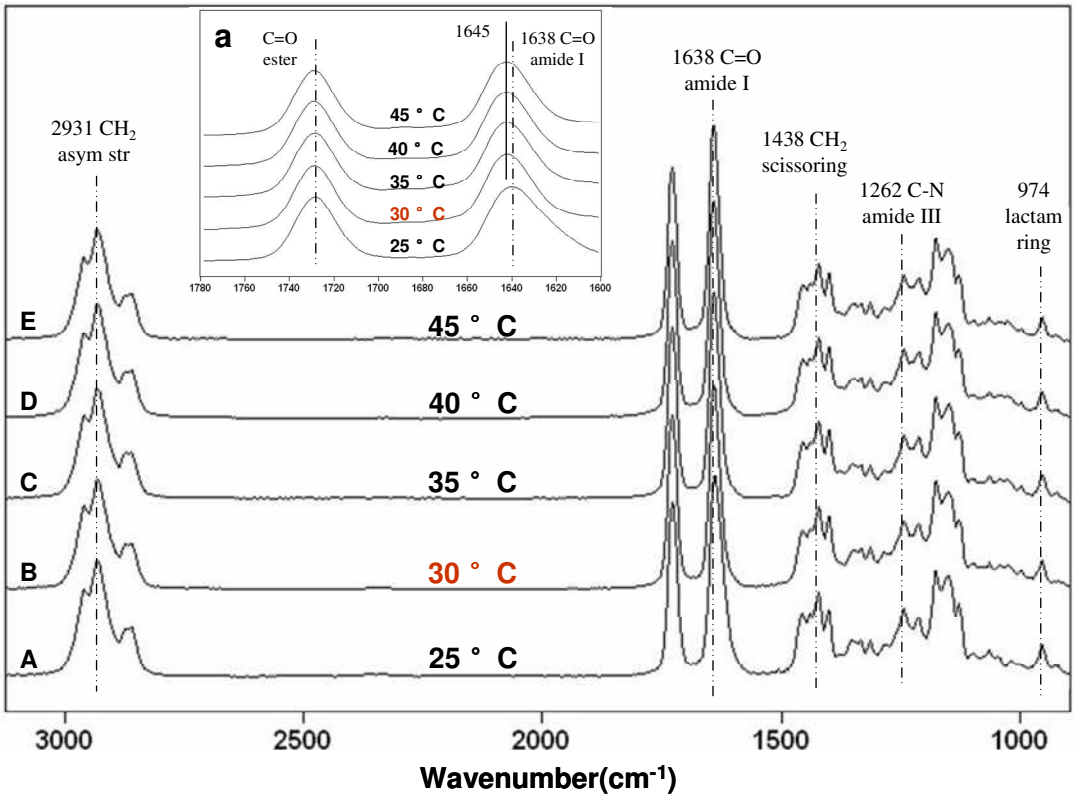

B Raman Spectra of p(VCl/nBA) as a Function of Temperature

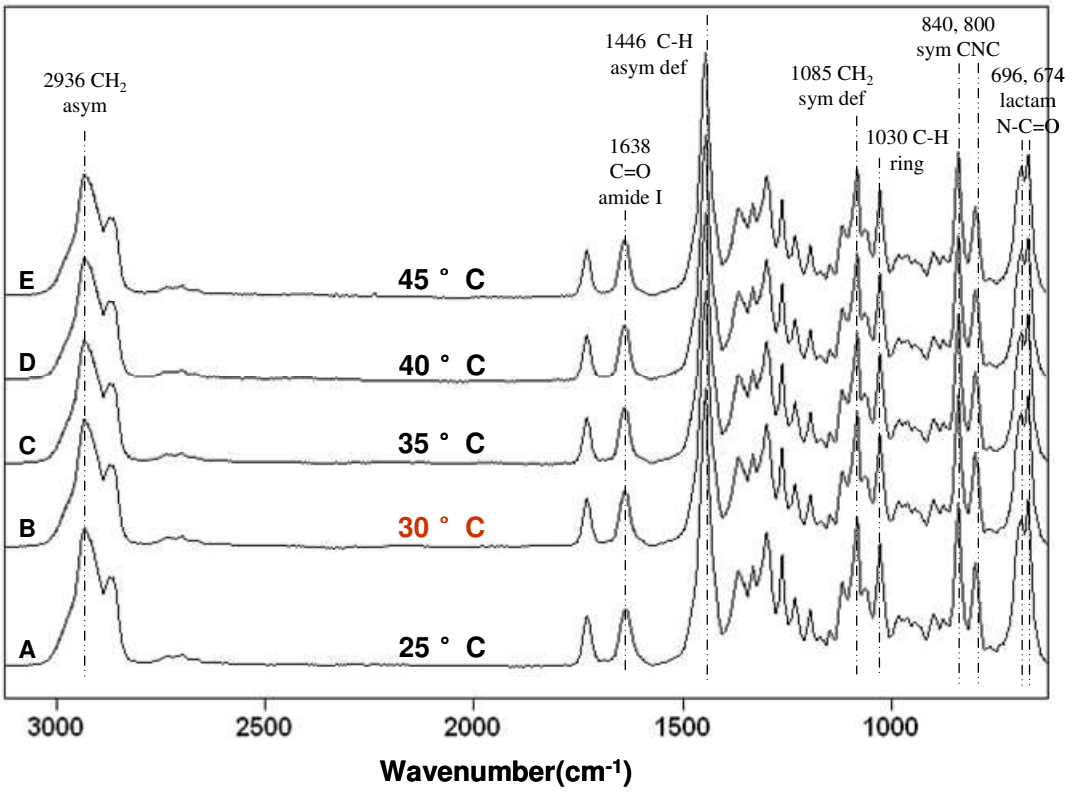

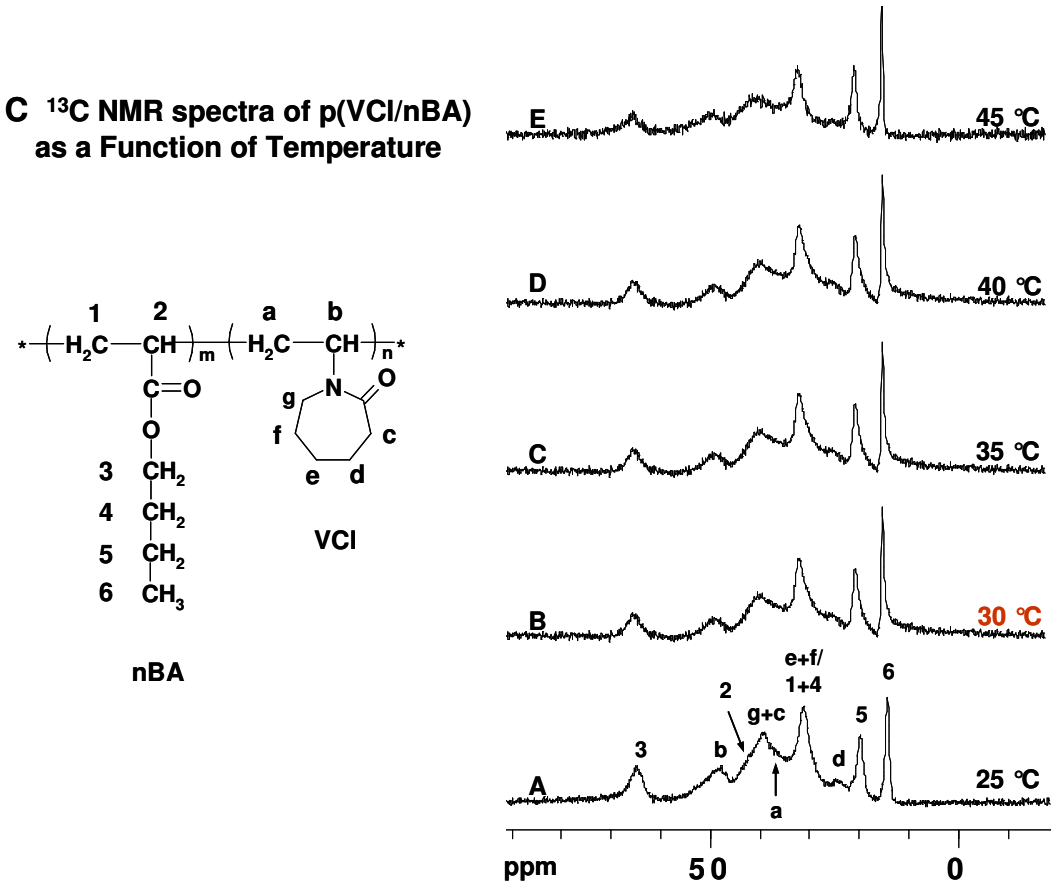

Figure S6. ATR FT-IR (A), Raman (B), and solid state ^{13}C NMR (C) spectra of p(VCl/nBA) recorded as a function of temperature; A-25 °C; B-30 °C; C-35 °C; D-40 °C; E-45 °C.

A IR Spectra of p(NIPMAm/nBA) as a Function of Temperature

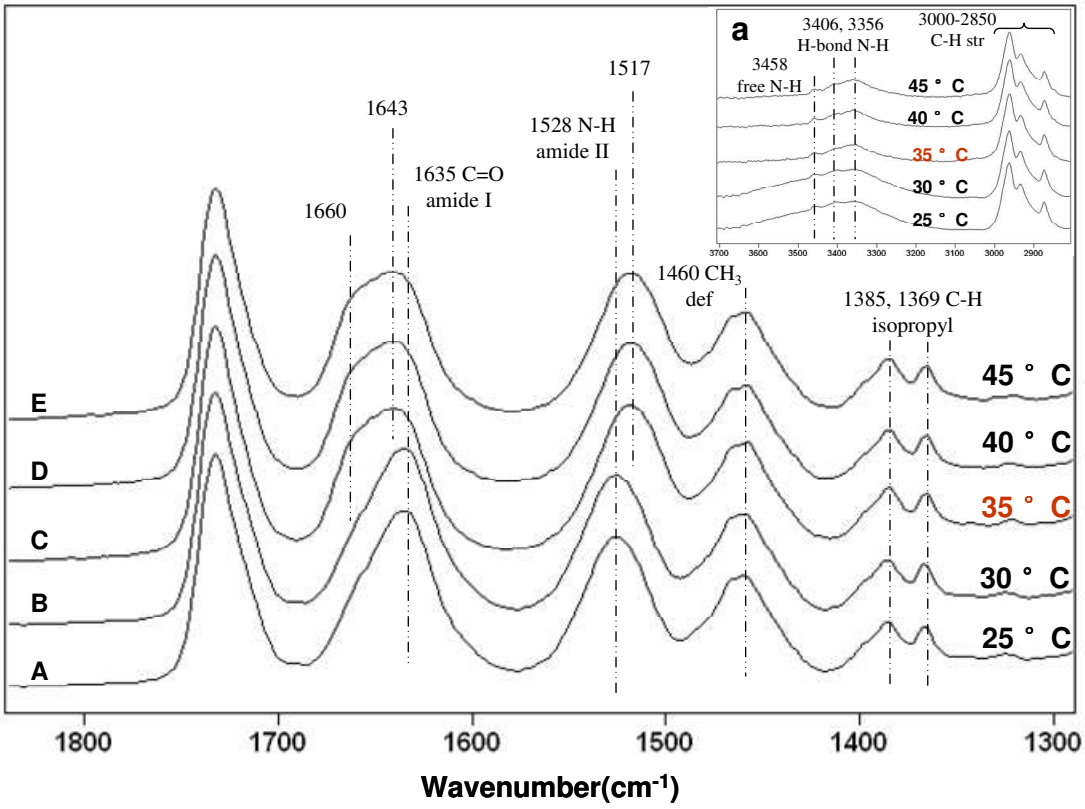

B Raman Spectra of p(NIPMAm/nBA) as a Function of Temperature

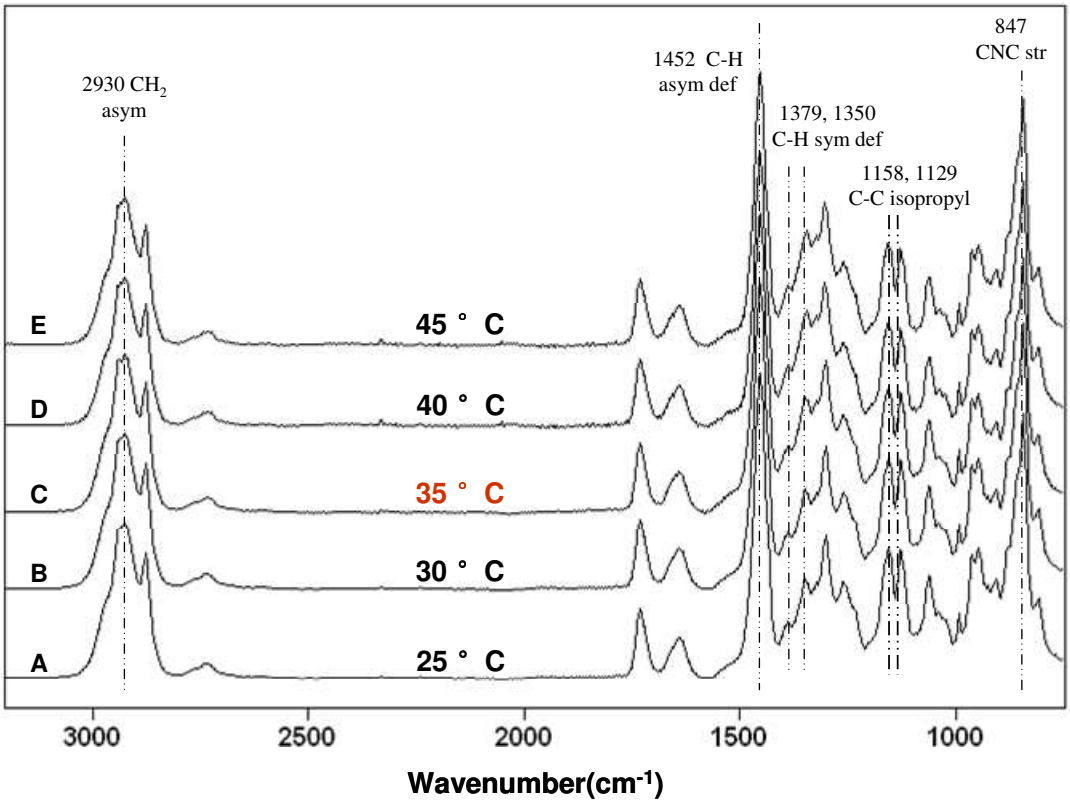

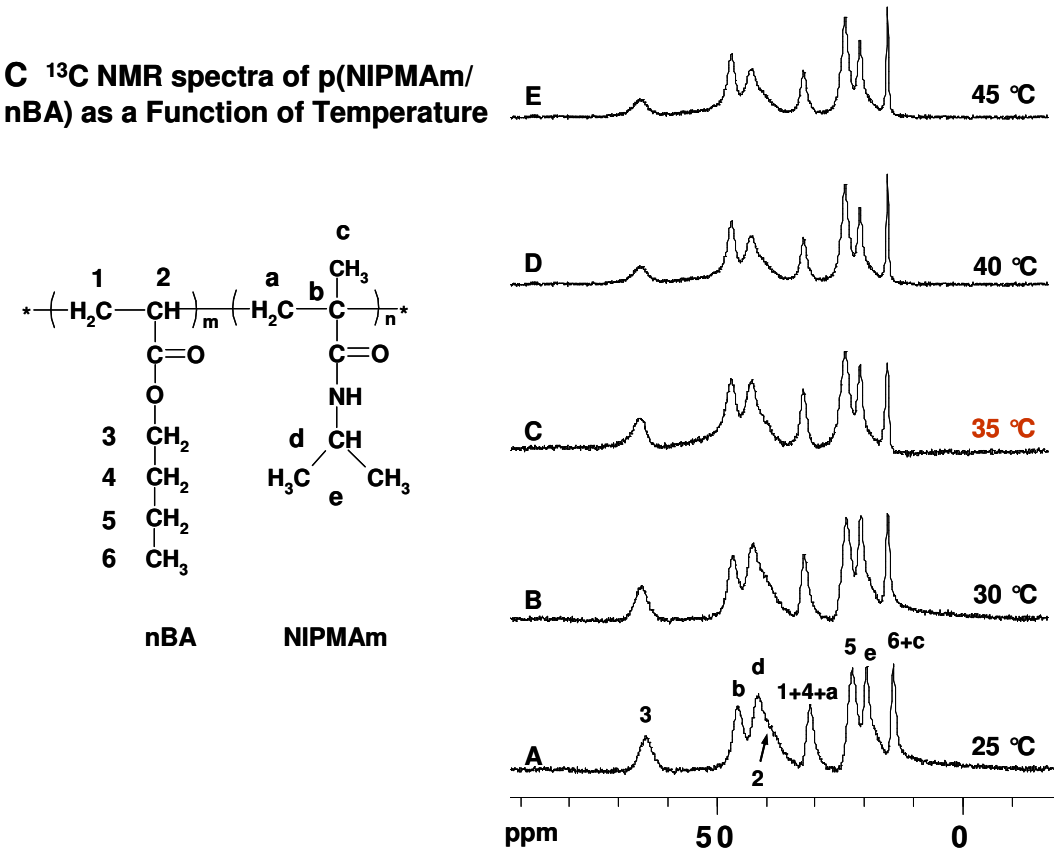

Figure S7. ATR FT-IR (A), Raman (B), and solid state ^{13}C NMR (C) spectra of p(NIPMAm/nBA) recorded as a function of temperature; A-25 °C; B-30 °C; C-35 °C; D-40 °C; E-45 °C.

A IR Spectra of p(DMAEMA/nBA) as a Function of Temperature

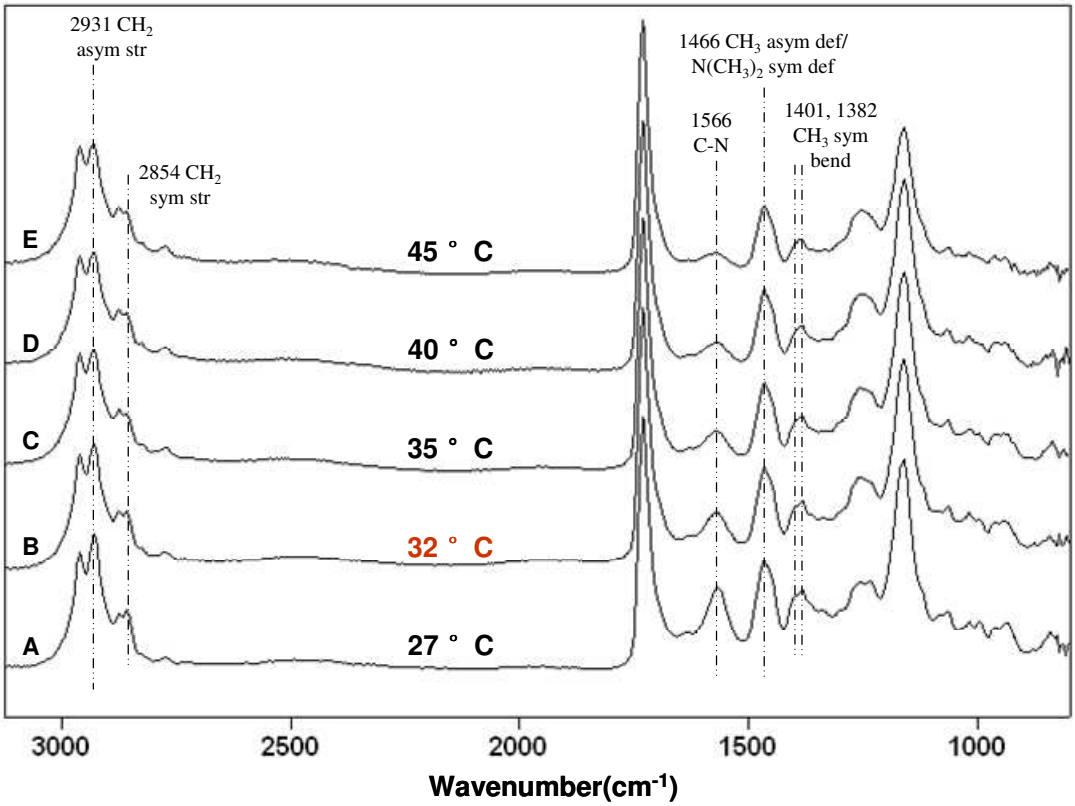

B Raman Spectra of p(DMAEMA/nBA) as a Function of Temperature

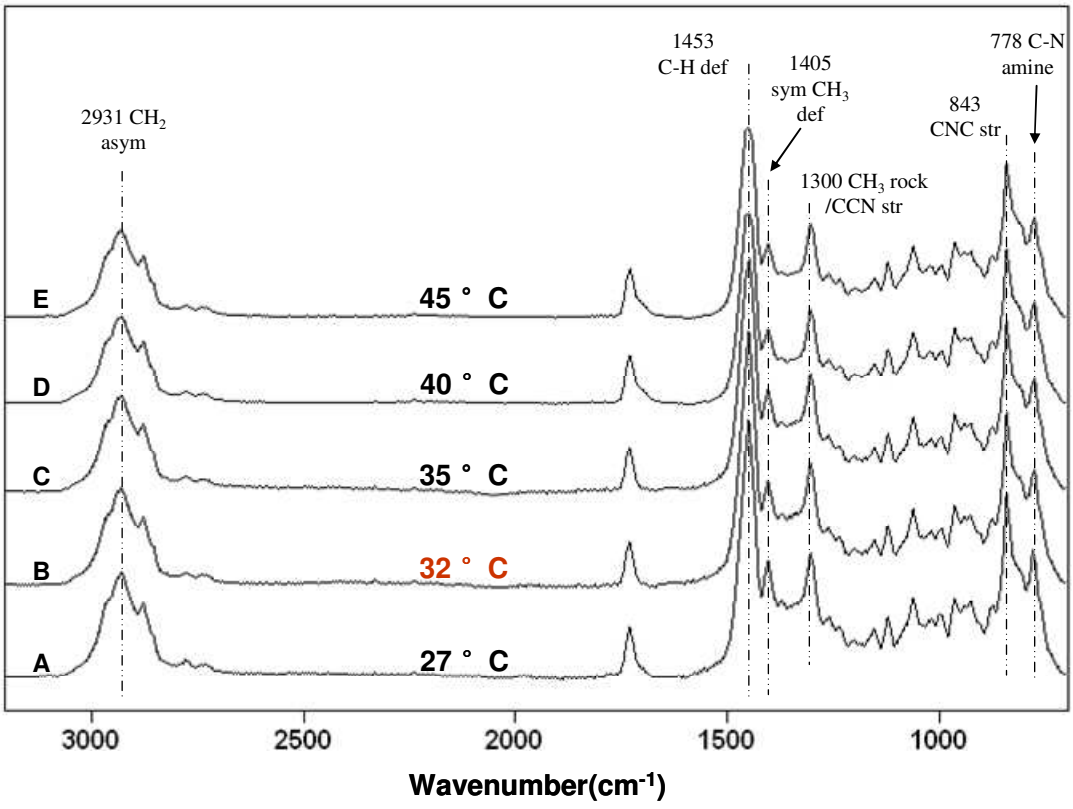

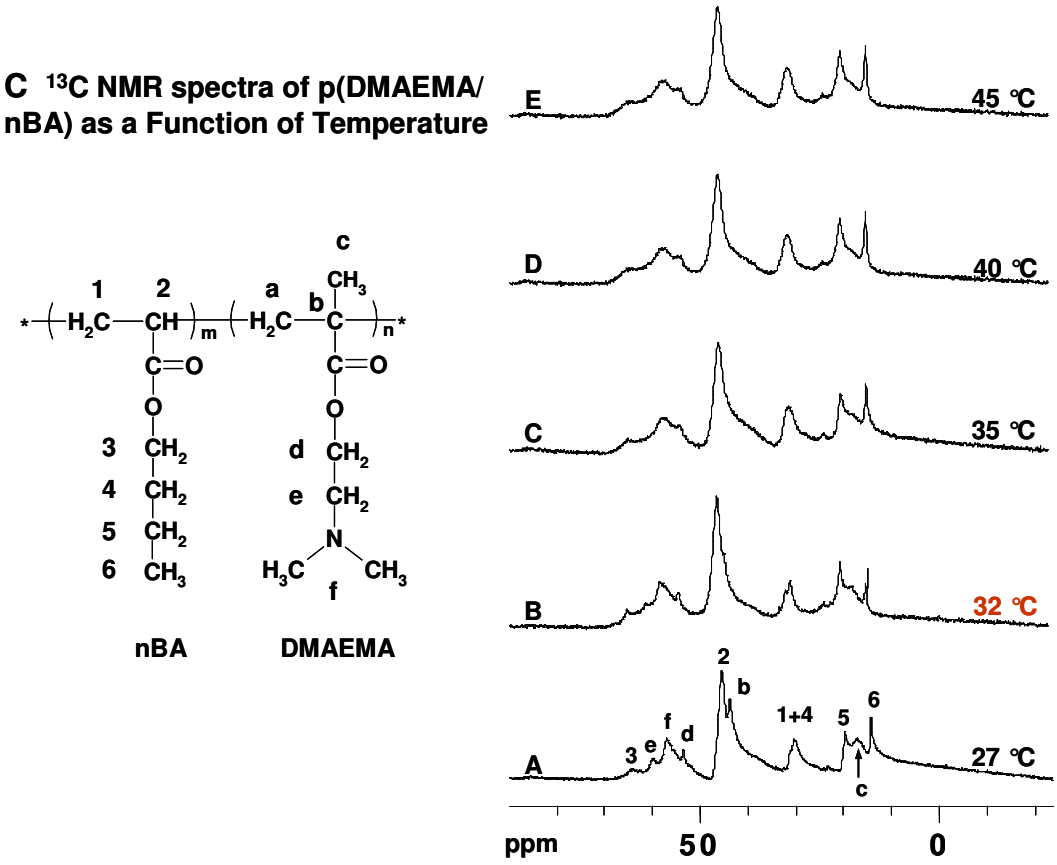

Figure S8. ATR FT-IR (A), Raman (B), and solid state ^{13}C NMR (C) spectra of p(DMAEMA/nBA) recorded as a function of temperature; A-27 °C; B-32 °C; C-35 °C; D-40 °C; E-45 °C.

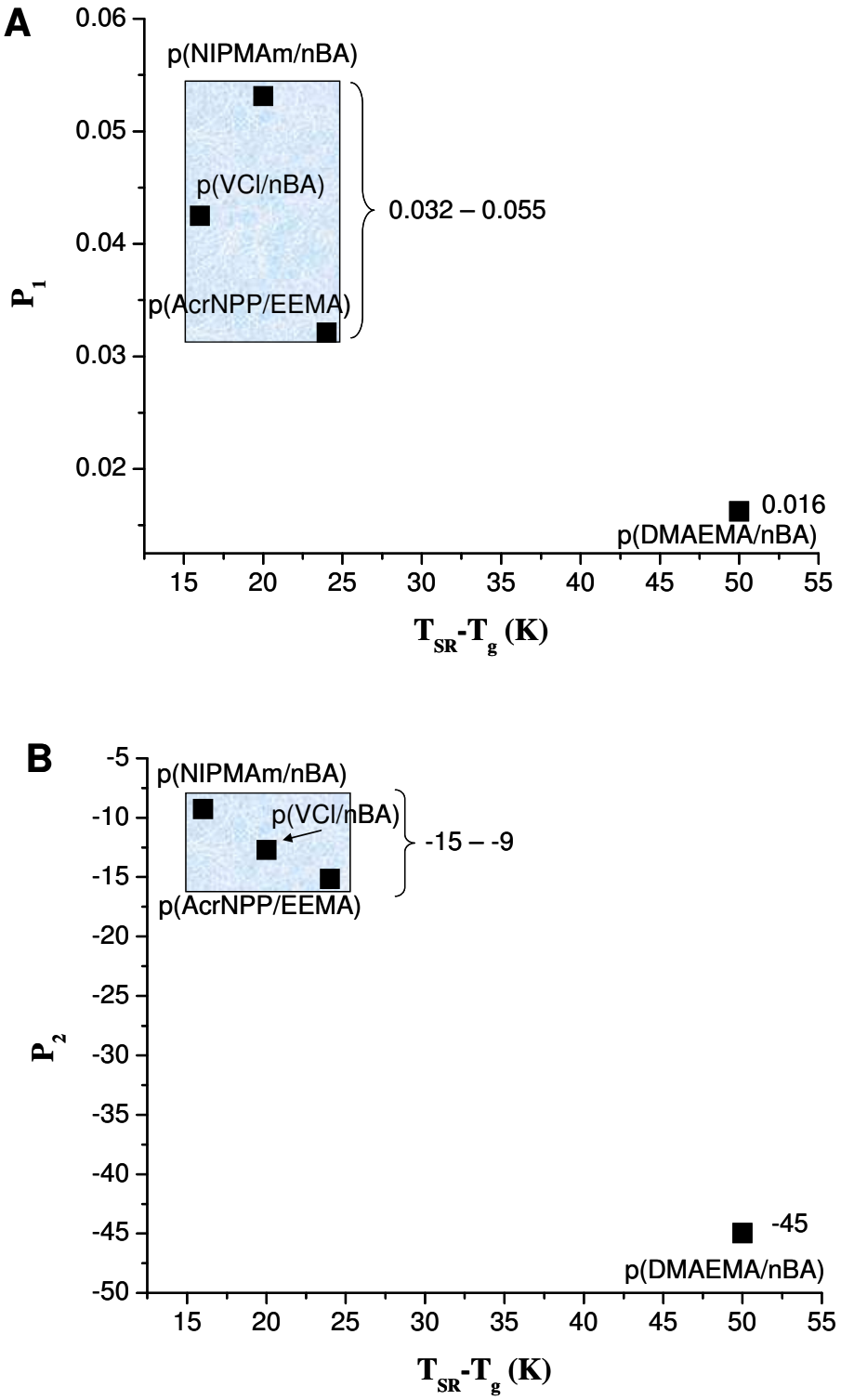

Figure S9. P_1 (A) and P_2 (B) values plotted as a function of (T_{SR}-T_g) for copolymers with 50/50 composition.

Reference

1. Gan, L. H.; Gan, Y. Y.; Deen, R. *Macromolecules* 2000, 33, 7893.
2. Coskun, M.; Barim, G.; Demirelli, K. *J. Macromol. Sci., Pure Appl. Chem.* 2006, 43, 83.
3. Chang, L.; Kong, X.; Wang, F.; Wang, L.; Shen, J. *Thin Solid Films* 2008, 516, 2125.
4. Lin-Vien, D.; Colthup, N. B.; Fateley, W. G.; Grasselli, J. G., *The Handbook of Infrered and Raman Characteristic Frequencies of Organic Molecules*. Acadenic Press: San Diego, 1991.
5. Pretsch, E.; Buhlmann, P.; Affolter, C., *Structure Determination of Organic Compound: Tables of Spectral Data*. 3rd ed.; Springer: New York, 2000.
6. Socrates, G., *Infrared and Raman Characteristic Group Frequencies: Tables and Charts*. 3rd ed.; John Wiely and Sons Ltd: New York, 2001.
7. Tiemblo, P.; Laguna, M. F.; Garcia, F.; Garcia, J. M.; Riande, E.; Guzman, J. *Macromolecules* 2004, 37, 4156.
8. Sanmathi, C. S.; Prasannakumar, S.; Sherigara, S. *Bull. Mater. Sci.* 2004, 27, 243.
9. Maeda, Y.; Nakamura, T.; Ikeda, I. *Macromolecules* 2002, 35, 217.
10. Misra, A.; Urban, M. W. *Macromolecules* 2009, 42, 7299.
11. Dybal, J.; Trchova, M.; Schmidt, P. *Vib. Spectrosc.* 2009, 51, 44.
12. Kim, D. J.; Lee, K.; Chi, Y. S.; Kim, W.; Paik, H.; Choi, I. S. *Langmuir* 2004, 20, 7904.
13. Liu, Q.; Yu, Z.; Ni, P. *Colloid Polym. Sci.* 2004, 282, 387.
14. Heijl, J.; Du Prez, F. *Polymer* 2004, 45, 6771.